Characterization of Excited States of Quinones and Identification of Their Deactivation Pathways

Arianna Barbafina, Loredana Latterini, Benedetta Carlotti, and Fausto Elisei*

Department of Chemistry and Centro di Eccellenza sui Materiali Innovativi Nanostrutturati (CEMIN), via Elce di Sotto 8, Perugia 06123, Italy

Received: December 11, 2009; Revised Manuscript Received: April 16, 2010

Femtosecond time-resolved transient absorption was used to investigate the properties of the excited states of *p*-benzoquinone derivatives: ubiquinone 0 (UQ_0), thermoquinone (TQ), and tetramethylbenzoquinone (TMBQ). To elucidate details of the deactivation pathways of quinones, experiments were carried out in solvents with different polarity by exciting the samples at 400 and 266 nm. The measurements carried out upon excitation centered at 400 nm pointed out that the $S_1 \rightarrow T_1$ intersystem crossing (ISC) is operative only for TMBQ, where the $T_2(\pi,\pi^*)$ state is likely below S_1. For UQ_0 and TQ, this decay process is not efficient because of the high energy of T_2 located above S_1. Instead, the lowest triplet state of UQ_0 was detected upon excitation at 266 nm, showing the involvement of an upper excited singlet state (S_n) in the ISC process.

Introduction

Excited states of naturally occurring quinones are of interest with respect to the degradative action of light upon biological materials, phosphorylation,[1] and the possibility of initiating electron transport in mitochondria by quinone light absorption.[2,3] In fact, quinones play important roles in electron transfer in bacteria,[4] photosystems of green plants, and mitochondria.[5]

Quinones possess both potent photodynamic action and the ability to undergo redox cycling, where they can produce radical oxygen species (ROS) via either oxidation of water or reduction of dioxygen.[6−8] Furthermore, quinones and their reduced derivatives act as electron donors and acceptors in photosynthesis, and it is possible that they act as electron shuttles in sunlit surface waters as well.[9]

Despite their biological importance, experimental data for free ubiquinones are limited. Upon absorption of a photon of light, ground-state molecules of quinone (Q) are first excited to the singlet state that undergoes rapid intersystem crossing (ISC) to form the excited triplet state (^{3}Q*).[10,11] ^{3}Q* can be quenched by molecular oxygen, regenerating Q and producing singlet oxygen,[12] or can decay directly to the ground state Q. Most photophysical and photochemical studies of quinones are related to the triplet excited state,[13] and little is known about its precursor, the excited singlet state.

To get more insight into the quinones properties induced upon light absorption, the primary decay processes of the excited electronic states of three *p*-benzoquinone derivatives were investigated. In particular, the benzoquinones under investigation were selected to compare the primary deactivation events that efficiently lead to a long living transient assigned to the lowest triplet state, in many benzoquinone derivatives, such as tetramethylbenzoquinone (TMBQ),[13] whereas other derivatives like ubiquinone and thermoquinone (TQ) do not produce long-living species in nanosecond laser flash photolysis experiments.[13]

In particular, in the present work, the excited states of ubiquinone 0 (UQ_0), TQ, and TMBQ formed upon excitation with 40 fs pulses having different excitation energy were detected and characterized in different solvents by ultrafast transient absorption measurements.

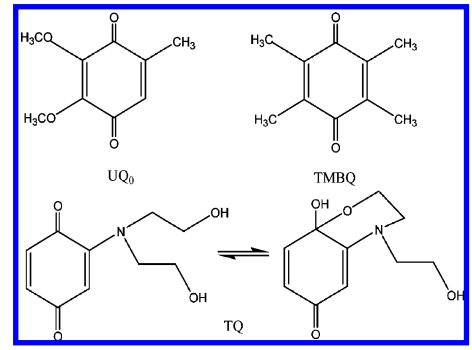

Figure 1. Chemical structure of investigated compounds.

Experimental Methods

Materials. The investigated compounds are shown in Figure 1. The substrates 2,3,5,6-tetramethyl-1,4-benzo-quinone (duroquinone, TMBQ) and 2,3-dimethoxy-5-methyl-*p*-benzo-quinone (UQ_0) were purchased from Sigma-Aldrich and used without further purification. Instead, 2-(*β*-hydroxyl-ethylamine)-1,4-benzoquinone (TQ) was synthesized as reported by Koenig[14,15] and modified for the crystallization step as indicated in Trotta et al.[16] TQ purity was checked via melting temperature (163−164 °C), NMR spectroscopy, UV−vis, and fluorescence spectroscopy.

TQ in solution exists as a tautomeric equilibrium between the ketonic and hemiketalic forms (Figure 1), the concentration of the open form being increased by the temperature.

All solvents (Fluka, spectrophotometric grade) were used as received. Phosphate buffer (PB) was used to adjust pH 7.2 in aqueous medium, where specified.

Absorption and Emission. Absorption spectra of the sample solutions were recorded by a Perkin-Elmer spectrophotometer (Lambda 800).

Quantum mechanical calculations were performed by use of the CAChe 7.5 software. Transition energies and oscillator strengths were obtained by the INDO/1 model, after geometrical

* Corresponding author. Tel: +39 075 5855588. Fax: +39 075 5855598. E-mail: elisei@unipg.it.

10.1021/jp911734x
Published on Web 04/28/2010

optimization of the molecular structure, with the density functional theory B3LYP/6-31G(d) model (Gaussian 03). In all cases, electronic excitations (singly excited) from the 20 highest occupied to the 20 lowest virtual molecular orbitals were used.

Fluorescence spectra and quantum yields were measured with a Fluorolog-2 (Spex, F112AI) spectrophotofluorimeter (mean deviation of three independent experiments, ca. 5% for ϕ_F) in solutions air-equilibrated (absorbance <0.1 at the excitation wavelength) by using anthracene in ethanol as standard, $\phi_F = 0.27$.[17]

The fluorescence lifetimes, τ_F (mean deviation of three independent measurements, ca. 5%), were measured by a Spex Fluorolog-τ2 system, which uses the phase-modulation technique (excitation wavelength modulated in the 1−300 MHz range; time resolution ca. 10 ps). The frequency−domain intensity decays (phase angle and modulation vs frequency) were analyzed with the Global Unlimited (rev.3) global analysis software.[18]

Laser Flash Photolysis. Nanosecond time-resolved measurements were carried out by use of a flash photolysis setup previously described (Nd/YAG Continuum, Surelite II, third harmonics, $\lambda_{exc} = 355$ nm, pulse width ca. 7 ns and energy ≤1 mJ pulse^{-1}).[19,20]

Femtosecond Measurements. Femtosecond pulses were generated by an amplified titanium−sapphire laser system (Spectra Physics, Mountain View, CA) that produces 1 W pulses of 40 fs centered at 800 nm with a repetition rate of 1 kHz.[21] Pump pulses centered at 400 were obtained by a second harmonic (SH) generation in a 500 μm β-barium-borate crystal. To generate the third harmonic (266 nm), the SH and residual fundamental pulses were overlapped in space and time on a third harmonic generator (THG) β-barium-borate crystal.

In the transient absorption set up (Helios, Ultrafast Systems), the pump pulses were passed through a chopper that cut out every second pulse and collimated to the sample in a 2 mm quartz cuvette. Probe pulses for optical measurements were produced by passing a small portion of 800 nm light through an optical delay line (with a time window of 1600 ps) and focusing into a 2 mm thick Ti/sapphire crystal to generate a white-light continuum in the 450−800 nm window. The white light was focused onto the sample, and the chirp inside the sample cell was corrected by measuring the laser-induced Kerr signal of the solvent. The apparatus response time is ∼150 fs.

Results and Discussion

$S_0 \rightarrow S_n$ Absorption Spectra. The absorption spectra of the investigated compounds were recorded at room temperature in several solvents with different polarity. In general, the spectra of these compounds show the main maximum in the UV region ($\varepsilon_{max} > 8000$ M^{-1} cm^{-1}) and a broad band at longer wavelengths ($\varepsilon_{max} < 1000$ M^{-1} cm^{-1}). The experimental absorption spectra can be compared with those predicted by quantum mechanical calculations (Table SI1 in the Supporting Information). The calculations with the INDO/1-CI method were first carried on *p*-benzoquinone (whose electronic excited states have been studied by using multiconfigurational second-order perturbation theory (CASPT2)[21]) and compared with experimental and theoretical data already reported in the literature.[22] Because these sets of data are in good agreement, the semiempirical model INDO/1-CI can be considered to be able to describe the spectral properties of the molecules here investigated and can be used to assign the nature of their transitions.

In general, quinones show the main absorption maxima at ∼250 nm and a bathochromic band with smaller absorption coefficients. The absorption spectra depend slightly on the solvent polarity; only the band placed at lower energies (due to the $S_0 \rightarrow S_3$ transition) increases its intensity and shifts toward longer wavelengths by increasing the solvents polarity (data not shown).

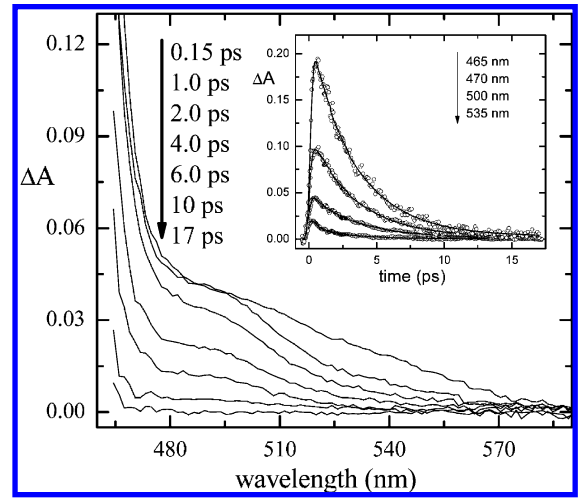

Figure 2. Time-resolved absorption spectra of UQ_0 in acetonitrile recorded at different delay times ($\lambda_{exc} = 400$ nm). Inset: kinetic decays of excited states of UQ_0 in acetonitrile at different wavelengths together with the best biexponential fittings of the experimental data ($\lambda_{exc} = 400$ nm).

Different spectral features were observed for TQ. In fact, its spectral properties are affected by the presence of a tautomeric equilibrium between open and closed forms (Figure 1). The UV−vis spectrum presents two absorption bands centered at 360 and 500 nm because of a ($\pi \rightarrow \pi^*$) and ($n \rightarrow \pi^*$) transition, respectively. The TQ absorption band centered at 500 nm is rather weak, and its intensity increases with the temperature. Because the quinonic form of TQ is favored by the increase in temperature, the band at 500 nm is assigned to the open form of the substrate.[16,23]

The investigated compounds did not show any fluorescence with the exception of TQ, whose weak emission ($\lambda_{max} \approx 510$ nm and $\phi_F = 1.5 \times 10^{-3}$ in acetonitrile) was ascribed to the hemiketalic form.[24]

Transient Absorption. *UQ_0*. Upon femtosecond laser excitation of UQ_0, a positive ΔA signal was recorded in the whole investigated range with a maximum below 450 nm. (See Figure 2 as an example.) The solvent does not significantly affect the band shape, but it influences the decay times.

The decay traces were analyzed in each solvent at different wavelengths. (See the inset of Figure 2, where the solid lines represent the best fittings obtained by biexponential functions convoluted with the instrumental response profile of Gaussian shape.) The global analysis also showed the presence of two exponential decays (a short-lived and a longer-lived component; S and L, respectively).

Moreover, no further absorptions replaced the S and L signals after their decay. This behavior is in agreement with nanosecond laser flash photolysis experiments carried out upon excitation at 355 nm, where no transients were detected.

Furthermore, through kinetic analysis, it was possible to state that the short-lived transient S was always formed within the laser pulse and it was precursor of the longer-lived L. Table 1 shows the corresponding time constants τ_S and τ_L that change in the range of 0.4−2.6 and 0.6−45 ps, respectively. It is evident that both τ_S and τ_L significantly decrease with increasing solvent polarity. In aqueous media, even though the decay traces at

TABLE 1: UQ_0 Excited States Lifetimes (Obtained by Transient Absorption upon Irradiation at 400 nm)[a]

solvent	ε @ 20 °C	τ_S (ps)	τ_L (ps)
water	80.1	0.42	0.63
PB (pH 7.2)	80.1	0.45	0.60
D_2O	79.8	0.50	0.68
DMSO	46.7	0.75	3.8
acetonitrile	37.0	0.50	3.6
methanol	33.6	0.60	3.3
ethanol	24.3	1.5	5.1
chloroform	4.81	1.5	7
toluene	2.38	1.1	14
1,4-dioxane	2.21	1.3	7.6
cyclohexane	2.02	2.6	45
n-hexane	1.89	2.0	40

[a] Dielectric constant of the solvent (ε) is also reported.

TABLE 2: UQ_0 Excited States Lifetimes (Obtained by Transient Absorption upon Excitation at 266 nm)

solvent	τ_S (ps)	τ_L (ps)	
acetonitrile	≤0.3	3.0	rest
cyclohexane	7.2	50	rest
n-hexane	4.0	34	rest

different wavelengths are well correlated by monoexponential functions, the decay lifetime depends on the wavelength of analysis. In fact, the signal recorded at longer wavelengths is formed within the laser pulse, whereas at shorter wavelengths, the growth is slower. This behavior is explained by the presence of two species with close lifetimes ($\tau_S \approx 0.4$ ps and $\tau_L \approx 0.6$ ps) so that the biexponential function of the decay kinetics was not able to improve the fitting.

The absorption spectra of S and L were determined by using the singular value decomposition (SVD) method, followed by global analysis of the experimental data (Figure SI1 in the Supporting Information). The S component shows a negative signal at wavelengths shorter than 510 nm and a positive absorption with a maximum at 540 nm in all solvents, except for cyclohexane, where the maximum is centered at ~600 nm; instead, the longer-lived transient shows a positive signal in the whole probed spectral range. These spectral properties are in agreement with a precursor−successor scheme, which involves the S → L step.

To evidence if there is a substantial effect of the excitation wavelength on the deactivation pathways of the excited states of UQ_0, as suggested by a comparison between our results and those previously obtained by Bensasson et al.[25] through nanosecond laser flash photolysis, experiments were carried out by exciting at 266 nm.

The results obtained by these investigations are shown in Table 2 and Figure 3. In fact, upon 266 nm excitation, UQ_0 was able to form a further species that does not decay in the temporal window under investigation. Therefore, in the employed solvents, the decay analysis revealed the presence of two transient species together with a residual absorption (S, L, and rest, respectively) whose spectral components are shown in Figure SI2 in the Supporting Information.

Taking into account the analysis of the data obtained upon excitation at 400 nm, L was ascribable to the lowest singlet state S_1, whereas S, which is a precursor of L, represents the decay of an upper singlet state (S_3, according to calculations) produced by direct excitation. The deactivation rate constants of UQ_0 were determined to be k_S ($= 1/\tau_S$) $\approx 10^{12}$ s^{-1} and k_L ($= 1/\tau_L$) $\approx 10^{10}-10^{12}$ s^{-1}. Taking also into account that steady-state irradiation did not show formation of photoproducts, these

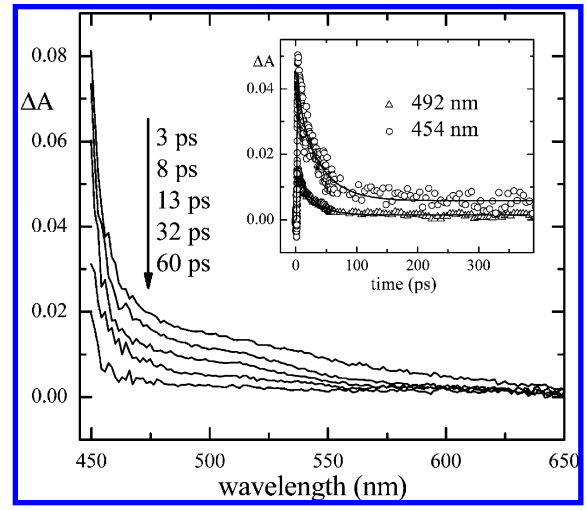

Figure 3. Time-resolved absorption spectra of UQ_0 in *n*-hexane recorded at different delay times ($\lambda_{exc} = 266$ nm). Inset: kinetic decays of excited states of UQ_0 in *n*-hexane at different wavelengths together with the best biexponential fittings of the experimental data ($\lambda_{exc} = 266$ nm).

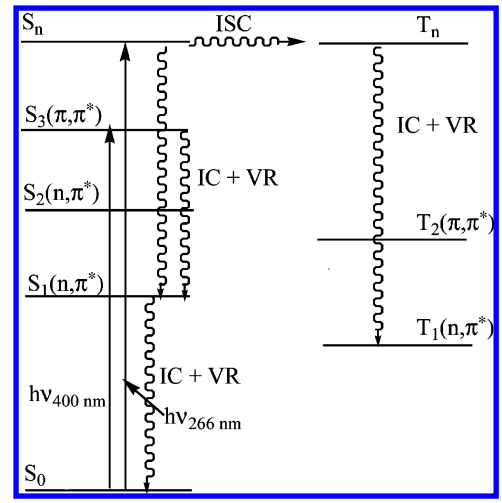

Figure 4. Relaxation processes of UQ_0.

rate constant values can be taken as a measure of the rate constants of the internal conversions (ICs) $S_3 \rightarrow S_1$ and $S_1 \rightarrow S_0$, respectively, combined with vibrational relaxations (VRs), which are represented in Figure 4. The decay process of S_1 is very fast, and it is greatly affected by the solvent polarity; in fact, k_L decreases by two orders of magnitude on going from water to *n*-hexane. This behavior, which reflects the rate of the $S_1 \rightarrow S_0$ transition (Fermi's golden rule[26]), may be explained by taking into account the effect of the solvent on the S_1 energy, which is destabilized by the solvent polarity, and by the mixing of the low lying states of different nature.

Upon irradiation at 266 nm, different deactivation pathways were observed. In fact, as reported above, the transient absorptions of S and L were replaced by a residual signal (rest) at long delay time. Analogously to the case of excitation at 400 nm, the transient L can be ascribed to the $S_1(v = 0) \rightarrow S_0$ transition. Instead, the S component, which showed slightly longer time constants than the ones recorded by excitation at 400 nm, reflects the decay channels that involve the S_n state and the triplet manifold (Figure 4) under these conditions.

Indeed, the rest signal recorded in solvents of different polarity (acetonitrile, cyclohexane, and *n*-hexane) upon excitation at 266 nm, shows a shape ascribable to the absorption tail

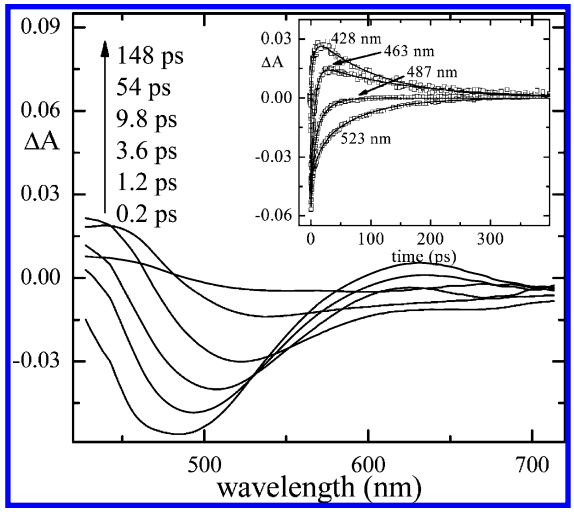

Figure 5. Time-resolved absorption spectra of TQ in methanol recorded at different delay times (λ_{exc} = 400 nm). Inset: kinetic decays of the excited states of TQ at different wavelengths together with the best biexponential fittings of the experimental data (λ_{exc} = 400 nm).

TABLE 3: TQ Excited States Lifetimes (Obtained by Transient Absorption upon Irradiation at 400 nm)

solvent	τ_S (ps)	τ_L (ps)
PB (pH 7.2)	8	55
DMSO	9	86
methanol	13.5	74
ethanol	22	105

of the lowest triplet state, T_1, already observed on a microsecond time scale for other quinones.[27,28] This assignment is also in agreement with nanosecond time-resolved experiments carried out upon excitation of UQ_0 at 266 nm, where it is shown that the lowest triplet state absorbs at ~420 nm and decays in hundreds of nanoseconds.[25]

These experimental data point out that at least in the case of UQ_0, a singlet−triplet ISC process can occur through an upper excited singlet state populated upon excitation at 266 nm.

TQ. The time-resolved absorption spectra of TQ were recorded in PB, DMSO, ethanol, and methanol (see Figure 5 as an example); in all of the solvents used, a broad negative band centered at 500 nm, due to the stimulated emission, was observed; moreover, the signal goes back to zero in hundreds of picoseconds with no indications of rest absorptions.

The decay traces were analyzed in each solvent at different wavelengths (Figure 5, inset). The global analysis of the experimental data also revealed the presence of two exponential decays (a short-lived and a longer-lived components, S and L, respectively) whose decay times are reported in Table 3. The kinetic analysis evidenced a precursor−successor model where decay times are in the 8−22 (S) and 55−110 ps (L) ranges; it has to be noted that both τ_S and τ_L decrease with the solvent polarity.

The spectral components S and L are shown in Figure SI3 (Supporting Information) in acetonitrile as an example. The S component shows a negative signal at wavelengths shorter than 480 nm and a positive absorption with a maximum at 620 nm; the absorption of the L component is almost the mirror image of S.

Furthermore, the decay lifetime of L (~80 ps) is very close to the fluorescence lifetime measured by the phase shift technique. Therefore, L is assigned to the lowest excited singlet state S_1 of TQ.

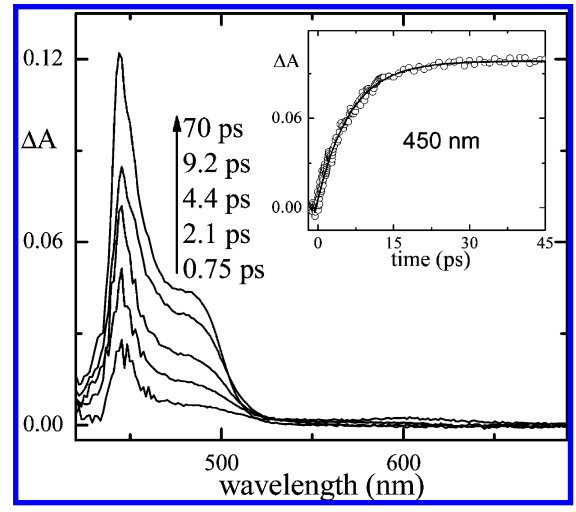

Figure 6. Time-resolved absorption spectra of TMBQ in acetonitrile recorded at different delay times (λ_{exc} = 400 nm). Inset: kinetic decay together with the best biexponential fittings of the experimental data (λ_{exc} = 400 nm).

TABLE 4: TMBQ Excited States Lifetimes Obtained by Transient Absorption upon Irradiation at 400 nm

solvent	τ (ps)	
DMSO	7.0	rest
acetonitrile	6.2	rest
methanol	6.5	rest
ethanol	6.0	rest
anisole	6.8	rest
toluene	6.9	rest

Taking into account the L assignment and the data reported in Table SI1 (Supporting Information), the transient S can be likely due to the relaxation from the Franck−Condon state (S_3), even if a contribution of the equilibration process in the excited state between the open and the closed forms of TQ cannot be excluded. The corresponding rate constant decreases by a factor two to three upon going from PB to ethanol.

TMBQ. The time-resolved absorption spectra of TMBQ are essentially due to the absorption of the transient species and to the depopulation of the ground state (Figure 6). In each solvent, the transient absorption spectra present a positive band in the 450−550 nm range (Table 4).

The 400 nm photoexcitation of TMBQ produces only one transient (S) together with a residual (rest) signal whose absorption spectra are shown in Figure SI4 in acetonitrile as an example. The dynamics of the excited states of TMBQ do not change upon 266 nm excitation.

The transient rest, recorded at long delay times, was assigned to the lowest triplet state of TMBQ because it presents an absorption spectrum very close to that already reported in the literature.[13] Instead, the transient S (detected in all of the investigated solvents) was assigned to the relaxation of the Franck−Condon state (S_3). which produces the T_1 state of TMBQ because it shows an absorption spectrum (Figure SI4, Supporting Information) that is the mirror image of the rest absorption. Taking into account that the triplet yield of TMBQ is close to unity,[13] the value of $1/\tau_S$ can be taken as a measure of the $S_1 \rightarrow T_1$ ISC rate constant (k_{ISC}). For TMBQ, the calculated k_{ISC} values are so high ($10^{10}-10^{12}$ s^{-1}) that a low energy difference between the triplet and singlet states and an efficient spin−orbit coupling (SOC) are required so that the spin forbidden processes can occur.[29] Moreover, SOC depends on the electronic configuration of the involved states (n,π^* or π,π^*);

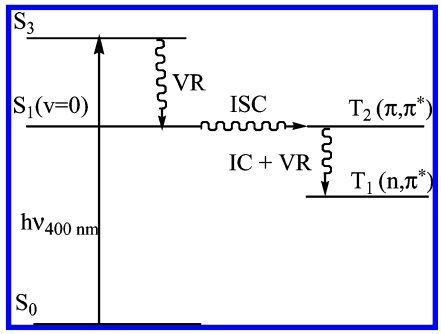

Figure 7. Relaxation processes of TMBQ.

in particular, SOC is very efficient between states with different configuration (n,π^* and π,π^*) and forbidden for states with the same nature. Therefore, to justify an ISC rate of 10^{12} s^{-1}, it is reasonable suppose that the ISC would occur between $S_1(n,\pi^*)$ and an intermediate state with π,π^* nature, which accelerates the spin-forbidden process. An upper triplet state T_2, with a π,π^* nature, which decays to T_1 (n,π^*) for IC, has already been invoked to explain the decay processes of singlet benzophenone (Figure 7). As a matter of fact, for several quinones, it has been demonstrated that S_1 is the spectroscopically and kinetically detectable precursor of T_1, whereas the state T_2, which can be involved in the ISC process, is too short to be detectable.[11]

The high values of recorded rate constants pointed out that for TMBQ, the SOC is an optimized process leading to an ultrafast ISC.[11,30]

Conclusions

The spectroscopic and kinetic investigations carried out with femtosecond time resolution were able to show the effect of the molecular structure and the excitation wavelength on the primary decay processes of *p*-benzoquinones. In fact, upon excitation at 400 nm, the main decay process of the excited singlet states of the symmetric TMBQ is the fast ISC, which does not occur in the case of the asymmetric UQ_0 and TQ. This behavior can be ascribed to the involvement of the T_2 state in the singlet−triplet ISC of TMBQ, which takes place in two steps: $S_1(n,\pi^*) \rightarrow T_2(\pi,\pi^*) \rightarrow T_1(n,\pi^*)$. For UQ_0 and TQ, the higher energy of T_2 (located above S_1) does not allow the ISC to be operative. Upon excitation at 266 nm, it was also demonstrated that an upper excited singlet state is involved in the singlet−triplet ISC of UQ_0.

Acknowledgment. We gratefully acknowledge the financial support of the Ministero per l'Università e la Ricerca Scientifica e Tecnologica (Rome, Italy) and the University of Perugia and the Fondazione Cassa di Risparmio di Perugia. We gratefully thank Dr. Massimo Trotta from the University of Bari (Italy), who kindly provided the molecules investigated in this work.

Supporting Information Available: Transitions of quinones calculated by INDO/1-CI (ZINDO) optimized by the B3LYP/6-31G(d) together with the experimental absorption properties (λ_{max} and ε_{max}) and amplitudes of the transients of UQ_0 in acetonitrile and *n*-hexane, TQ in methanol, and TMBQ in MeCN obtained by SVD and global analysis (λ_{exc} =400 nm). This material is available free of charge via the Internet at http://pubs.acs.org.

References and Notes

(1) Avron, M. *Current Topics in Bioenergetics*; Sanadi, D. R., Ed.; Academic Press: New York, 1967; Vol. II.
(2) Rich, P. R.; Bendall, D. S. *FEBS Lett.* **1979**, *105*, 189.
(3) Rich, P. R. *Photosynth. Res.* **1985**, *6*, 335.
(4) Okamura, M. Y.; Feher, G. *Adv. Photosynth.* **1995**, *2*, 577.
(5) Nohl, H.; Gille, L.; Staniek, K. *Ann. N. Y. Acad. Sci.* **1998**, *854*, 394.
(6) Lang, K.; Wagnerova, D. M.; Stopka, P.; Damerau, W. *J. Photochem. Photobiol., A* **1992**, *67*, 187.
(7) Alegría, A. E.; Ferrer, A.; Santiago, G.; Sepúlveda, E.; Flores, W. *J. Photochem. Photobiol., A* **1999**, *127*, 57.
(8) Görner, H. *Photochem. Photobiol. Sci.* **2006**, *5*, 1052.
(9) Steinberg-Yfrach, G.; Rigaud, J.; Durantini, E. N.; Moore, A. L.; Gust, D.; Moore, T. A. *Nature* **1998**, *392*, 479.
(10) Turro, N. J. *Modern Molecular Photochemistry*; University Science Books: Sausalito, CA, 1991.
(11) Hubig, S. M.; Bockman, T. M.; Kochi, J. K. *J. Am. Chem. Soc.* **1997**, *119*, 2926.
(12) von Sonntag, J.; Mvula, E.; Hildenbrand, K.; von Sonntag, C. *Chem.−Eur. J.* **2004**, *10*, 440.
(13) Barbafina, A.; Elisei, F.; Latterini, L.; Milano, F.; Agostiano, A.; Trotta, M. *Photochem. Photobiol. Sci.* **2008**, *7*, 973.
(14) Koenig, K. H. *Chem. Ber.* **1959**, *92*, 257.
(15) Koenig, K. H.; Letsch, G. *Chem. Ber.* **1959**, *92*, 1789.
(16) Trotta, M. In *Photosynthesis: Mechanisms and Effects*; Garab, G., Ed.; Kluwer Academic: Boston, 1998; Vol. II.
(17) Eaton, D. F. In *Handbook of Organic Photochemistry*; Scaiano, J. C., Ed.; CRC Press: Boca Raton, FL, 1989; Vol. I, pp 231−239 and references therein.
(18) Beechem, J. M.; Gratton, E.; Ameloot, M.; Kutson, J. R.; Brand, L. In *Fluorescence Spectroscopy: Principles and Techniques*; Lakowicz, J. R., Ed.; Plenum Press: New York, 1988; Vol. I and references therein.
(19) Görner, H.; Elisei, F.; Aloisi, G. G. *J. Chem. Soc., Faraday Trans.* **1992**, *88*, 29.
(20) Romani, A.; Elisei, F.; Masetti, F.; Favaro, G. *J. Chem. Soc., Faraday Trans.* **1992**, *88*, 2147.
(21) Barbafina, A.; Amelia, M.; Latterini, L.; Aloisi, G. G.; Elisei, F. *J. Phys. Chem. A* **2009**, *113*, 14514.
(22) Pou-Amerigo, R.; Merchan, M.; Orti, E. *J. Chem. Phys.* **1999**, *110*, 9536.
(23) Berg, H.; Zuman, P. *J. Chem. Soc., Perkin Trans.* **2000**, *2*, 1459.
(24) Trotta, M.; Bozzi, A.; Barisano, D.; Della Monica, M. *J. Mol. Liq.* **1999**, 261.
(25) Amouyal, E.; Bensasson, R. V.; Land, E. J. *Photochem. Photobiol.* **1974**, *20*, 415.
(26) Klessinger, M.; Michl, J. *Excited States and Photochemistry of Organic Molecules*; VHC: New York, 1995.
(27) Gschwind, R.; Haselbach, E. *Helv. Chim. Acta* **1979**, *62*, 941.
(28) Kemp, D. R.; Porter, G. J. *J. Chem. Soc. D* **1969**, *18*, 1029.
(29) Unett, D. J.; Caldwell, R. A. *Res. Chem. Intermed.* **1995**, *21*, 665.
(30) Khudyakov, I. V.; Serebrennikov, Y. A.; Turro, N. J. *Chem. Rev.* **1993**, *7*, 399.

JP911734X